Chiral Lanthanide Emissive LB Films

DOI: 10.1002/anie.200((will be filled in by the editorial staff))

First examples of circular polarized lanthanide luminescence from Langmuir-Blodgett films formed from optically active and amphiphilic Eu(III) based self-assembly complexes

Jonathan A. Kitchen[*], *Dawn E. Barry, Laszlo Mercs, Martin Albrecht, Robert D. Peacock, and Thorfinnur Gunnlaugsson*[*]

The development of functional nanomaterials and supramolecular systems is an active area of research, particularly for molecular recognition/sensing, catalysis, optical devices, and magnetically active compounds for switching and data storage.[1-9] Whilst much attention has been focused on transition metal based supramolecular systems[10-11], there has been a recent insurgence of lanthanide based systems.[12-14] These ions possess rich coordination environments and unique physical properties such as long lived and long wavelength emission in the visible or the NIR regions, as well as magnetic properties, which have been exploited for use in the developments of MRI contrast agents. Hence, these properties make them ideal and highly desirable candidates for the formation of functional supramolecular systems.[15-16] The development of supramolecular assemblies that can be further organized into functional devices is also of great current interest. This can be archived by covalently attaching appropriate ligands and complexes to nano-particles or flat surfaces; through the formation of polymers or by forming thin films using Langmuir-Blodgett (LB) techniques.[17] Herein we describe out efforts in bridging these two areas of research by employing lanthanide directed synthesis (using ligands **1** and **2**) in the formation of chiral luminescent lanthanide amphiphilic complexes, and their use in the formation of LB films, the properties of which can be probed by using circular polarized luminescence (CPL). The ligands were designed to include a terdentate coordination pocket with a closely associated sensitizing antenna (i.e. the *R*- or *S*-naphthylamine moieties) for the lanthanide ions such as Eu(III) and Tb(III); an approach that has been extremely successful for the development of luminescent supramolecular self-assembly structures such as chiral 'bundles'[18] and di-lanthanide triple stranded helicates.[19-21] Additionally, a long hydrophobic hexadecyl chain was included, to allow for the formation of Langmuir-Blodgett films. Ligands **1** and **2** were prepared in yields of 74% and 82%, respectively, by employing EDCI·HCl peptide coupling reactions between the *R*- and the *S*- isomers of precursors **3** and **4**, respectively,[18-20] and *N*-hexadecylamine (Figure 1). These were characterized using conventional methods (See Supporting Information); as well as by using circular dichroism (CD) spectroscopy, which confirmed that the compounds were isolated as a pair of enantiomers (See Supporting Information Fig. S1). Moreover, rod shaped single crystals were obtained from the slow evaporation of CH_2Cl_2/CH_3CN solution of both ligands allowing for solid state crystal structure analysis of both. The resulting X-ray structure of **1** was determined at 108 K and is shown in Fig. 1 (See also Supporting Information S2, S3 and Table S1). The ligand crystallized in the chiral monoclinic space group $P2_1$ and contained two crystallographically independent molecules in the asymmetric unit. One molecule has a relatively *trans* co-planar chain configuration (straight chain), whilst the other forms somewhat of a square through 'kinks' in the chain. The two independent molecules pack into dimers through classic NH···O hydrogen bonding and offset face to face π···π stacking (Fig. 1) where the pyridyl group of the straight chain compound sits inside the square adopted by the bent chain compound. Complexes of **1** and **2** were formed and studied using Nd(III), Sm(III), Eu(III), Tb(III), Dy(III), Yb(III) and Lu(III). However, this communication only focuses on the Eu(III) complexes, where $\mathbf{1_3Eu}$ and $\mathbf{2_3Eu}$ ($[Eu(\mathbf{L})_3](CF_3SO_3)_3$) were prepared from **1** and **2**, respectively, by reacting with $Eu(CF_3SO_3)_3$

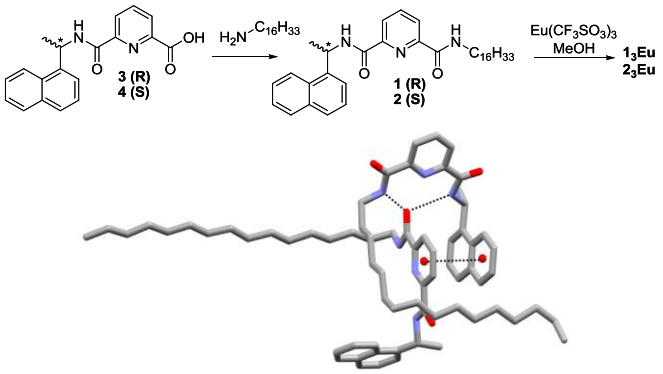

Figure 1. Synthesis of **1** (R), **2** (S) and their corresponding Eu(III) complexes $\mathbf{1_3Eu}$ and $\mathbf{2_3Eu}$. (a): EDCI·HCl, HOBt, THF, TEA, RT. Perspective view of the crystal structure of **1**. Dashed lines indicate inter-molecular interactions (N-H···O hydrogen bonding, and π···π stacking). Hydrogen atoms have been omitted for clarity.

[*] Prof. T. Gunnlaugsson, Dr. J. A. Kitchen and Ms D. E. Barry
School of Chemistry, Centre for Synthesis and Chemical Biology
Trinity College Dublin
College Green, Dublin 2, Ireland
E-mail: gunnlaut@tcd.ie and jkitchen@tcd.ie

Dr. L. Mercs and Prof. M. Albrecht
School of Chemistry and Chemical Biology
University College Dublin
Belfield, Dublin 4, Ireland

Prof. R. D. Peacock
School of Chemistry
Joseph Black Building, University of Glasgow
Glasgow, G12 8QQ

[**] We thank the Science Foundation Ireland (SFI PI Award 2010 (TG), SFI RFP Awards 2008 and 2009 (TG), the Irish Research Council for Science, Engineering & Technology (IRCSET, Postdoctoral Fellowship to JAK) and the European Research Council (StG 208561, MA) for financial support. We would like to thank particularly Dr Tom McCabe for assistance in collecting X-ray data.

Supporting information for this article is available on the WWW under http://www.angewandte.org or from the author.

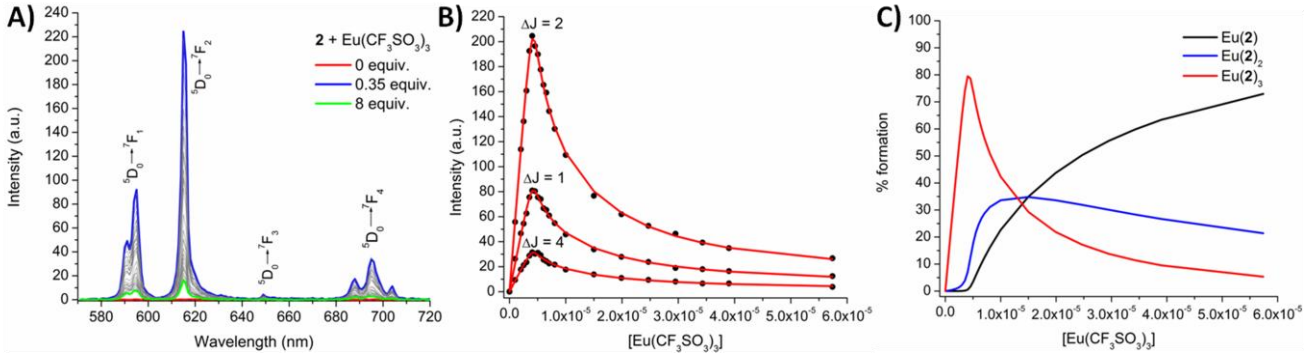

Figure 2: **A)** The overall changes in the Eu(III) phosphorescence spectra upon titrating **2** with $Eu(CF_3SO_3)_3$ (0 to 10 equivalents) in MeCN at RT. **B)** Experimental binding isotherms for the changes in the Eu(III) luminescence spectra upon titrating **2** with $Eu(CF_3SO_3)_3$ in MeCN at RT and their corresponding fit by means of SPECFIT (—). **C)** Speciation-distribution diagram obtained from the fit.

in 3:1 stoichiometry in methanol for 10 minutes under microwave irradiation. The pale yellow solutions were then subjected to vapor diffusion of diethyl ether yielding white solids; which under a UV lamp gave rise to typical red emission arising from the Eu(III) centre. Elemental analysis confirmed the formation of the desired products $\mathbf{1_3Eu}$ and $\mathbf{2_3Eu}$, whereas ESMS gave dominantly the *m/z* for the formation of $\mathbf{1_2Eu}$ and $\mathbf{2_2Eu}$.

The photophysical properties of $\mathbf{1_3Eu}$ and $\mathbf{2_3Eu}$ were evaluated in CH_3CN, MeOH, H_2O and D_2O solutions (See Supporting Information Figures S4 and S5 for some of these). The UV-Vis absorption spectrum of these complexes was dominated by an absorption assigned to the naphthalene $\pi \rightarrow \pi^*$ antenna with λ_{max} = 281 nm, and by the n $\rightarrow \pi^*$ transition of the central pyridyl unit. Excitation of the naphthalene antennae at 281 nm gave rise on both occasions to Eu(III) centered luminescence indicating effective sensitization of the $^5D_0$ excited state and subsequent deactivation to the ^7F_J states with line-like emission bands observed at 580 nm ($^5D_0 \rightarrow {}^7F_0$), 595 nm ($^5D_0 \rightarrow {}^7F_1$), 615 nm ($^5D_0 \rightarrow {}^7F_2$), 650 nm ($^5D_0 \rightarrow {}^7F_3$) and 695 nm ($^5D_0 \rightarrow {}^7F_4$). The coordination numbers of $\mathbf{1_3Eu}$ and $\mathbf{2_3Eu}$ were evaluated by determination of the number of water molecules bound to the Eu(III) centre, the hydration state (*q*), by monitoring their excited-state decay in H_2O and D_2O, respectively, in which these complexes were only sparingly soluble. For both, a *q* value of ~0 was determined for these complexes (See Supporting Information Table S2 and Figures S6 and S7) indicating that they were coordinatively saturated in aqueous solutions.

The formation of $\mathbf{1_3Eu}$ and $\mathbf{2_3Eu}$ was next observed in solution by monitoring the changes in the absorption spectra of **1** and **2** and in the evolution of the Eu(III) centered luminescence upon titration with $Eu(CF_3SO_3)_3$ in CH_3CN at room temperature. The latter method is an ideal way of observing the formation of these desired self-assemblies, as the population of the Eu(III) $^5D_0$ excited state would only be observed upon sensitization from the ligands, i.e. via the antennae effect. The overall changes observed in the Eu(III) emission for **2** are shown in Figure 2A, where all of the characteristic $^5D_0 \rightarrow {}^7F_{1\text{-}4}$ Eu(III) emission bands are observed upon formation of the self-assembly complex in solution. Analyzing the emission intensities of $^5D_0 \rightarrow {}^7F_{1\text{-}4}$ as a function of added Eu(III) equivalents reveals that the emission rapidly increases to a maximum at ca. 0.35 equiv., after which it decreases and begins to plateau after the addition of ~1 equiv. of Eu(III) (See Supporting Information Fig. S8 and S9). In order to gain a better understanding of the formation of these species in solution these changes were further analyzed by fitting the global luminescence changes using non-linear regression analysis (using the software SPECFIT) to various L:Eu stoichiometries. The fitting of the changes observed in Figure 2A are shown in Figure 2B (See Supporting Information Fig. S10 and S11 and Table S3 for the fitting and the binding constants obtained for the analysis of **1**). On both occasions good fits were observed as demonstrated for the analysis of **2** in Figure 2B, for the changes in ΔJ = 1, 2 and 4, from which the formation of $\mathbf{2_3Eu}$ in ca. 80% yield was confirmed after addition of ca. 0.3 equiv. Eu(III), with binding constants of logβ = 19.9 (±0.2). Concurrently, the analysis for **1** showed similar luminescent behavior, and the self-assembly $\mathbf{1_3Eu}$ was formed with a comparable binding constant logβ of 20.4 (±0.2). On further addition of Eu(III) the equilibrium for both systems was displaced towards that of a species with the stoichiometry [Eu(**L**)$_2$]; which after the addition of ca. 0.5 equiv. of Eu(III), were formed in 35 and 45 % yields, respectively, with binding constants of logβ = 13.3 (±0.2) and 14.1 (±0.2). On yet further addition of Eu(III), these equilibriums were displaced towards a new species, [Eu(**L**)], which became the predominant species after the addition of ~1.5 equiv. of Eu(III).

The solution formation of $\mathbf{1_3Eu}$ and $\mathbf{2_3Eu}$ was also observed by monitoring the changes in the absorption spectra, and by fitting the resulting global changes using non-liner regression analysis. In particular the changes in the absorbance bands at 207 nm, 223 nm and 281 nm were analyzed (See Supporting Information Figures S12 and S13 and Table S3). These changes gave rise to similar results as obtained from the analysis of the changes in the Eu(III) emission; the formation of the [Eu(**L**)$_3$] was confirmed after addition of 0.3 equiv. Eu(III), in ca. 85 % yield, with a binding constant of logβ of 20.9 (±0.3). Similarly, analysis of the changes observed for **1**, gave logβ of 20.5 (±0.3). Moreover, the formation of the [Eu(**L**)$_2$] species at ca. 0.5 equiv. of Eu(III) was also confirmed, in 45 and 35% yields for **1** and **2**, respectively, with logβ of 13.8; while upon further adaptations of Eu(III) resulted in the formation of the 1:1 stoichiometry [Eu(**L**)].

Using both CD and CPL, of $\mathbf{1_3Eu}$ and $\mathbf{2_3Eu}$ (See Supporting Information Figures S14 and S15, respectively) in CH_3CN confirmed the enantiomeric nature of these complexes. For the former, the CD spectra of $\mathbf{1_3Eu}$ and $\mathbf{2_3Eu}$ were significantly different to that seen for **1** and **2**, respectively, particularly for the naphthalene transitions (See Supporting Information Fig. S1 and S14). Importantly, both systems gave rise to Eu(III) centered CPL spectra, upon excitation of the naphthalene antennae, where all of the $^5D_0 \rightarrow {}^7F_{1\text{-}4}$ transitions were observed; clearly demonstrating that the Eu(III) ion was sitting within a chiral environment, where the handedness of the ligand dictated the handedness of the chiral emission (CPL) from the metal ion. This is evident from Figure S15, which shows a negative band for the ΔJ = 1 transition and a positive band for ΔJ = 2 nm for $\mathbf{1_3Eu}$; but these were found to be of opposite signs for $\mathbf{2_3Eu}$ confirming their formation as an enantiomeric pair. Comparison of these CPL spectra with those obtained previously in our laboratory using the symmetrical and chiral di-naphthalene amide analogue of **3** and **4**, for which the crystal structures of the 3:1 complexes are known,[18] allowed us to assign the absolute stereochemistry of these self-assemblies as Δ and Λ using **1** and **2**, respectively. Moreover, from these spectra, the luminescence dissymmetric factor g_{lum} was determined, which for $\mathbf{1_3Eu}$ gave g_{lum}

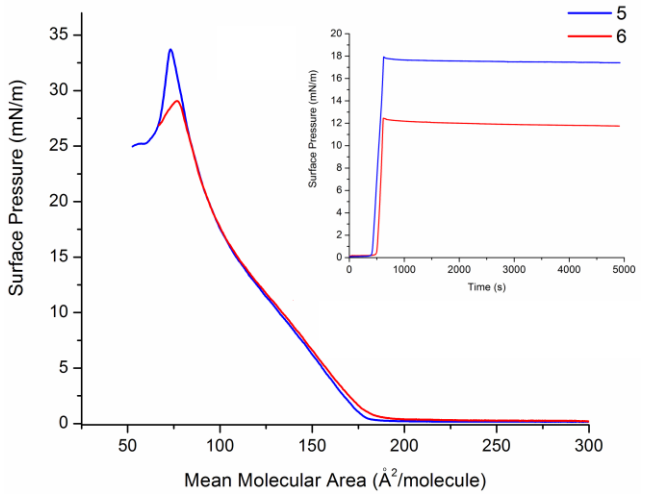

Figure 3. Pressure-area isotherms; inset shows pressure-time profiles for Langmuir films of **1_3Eu** (blue) and **2_3Eu** (red).

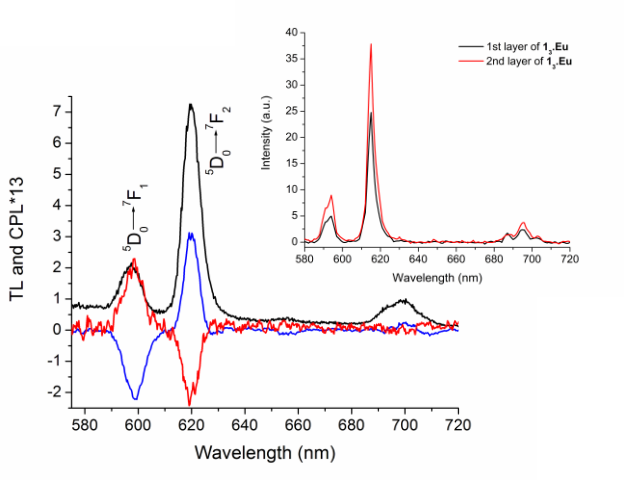

Figure 4. Total luminescence from **1_3Eu** (black) and CPL spectra from monolayers of **1_3Eu** (blue) and **2_3Eu** (red) on Quartz slides. *Inset:* The Eu(III) centered emission recoded of the Langmuir-Blodgett films after one and two emersions of **1_3Eu**.

= -0.177 and 0.106 for the ΔJ = 1 and 2 transitions, respectively (being g_{lum} = 0.176 and -0.102 for **2_3Eu**). The former, is close to that determined for the Eu(III) complex of the aforementioned symmetric analogue of **3** (g_{lum} = 0.28)[18], while for the ΔJ = 2 transition, g_{lum} was almost five times smaller (g_{lum} = 0.50)[18]. This might reflect the unsymmetical nature of **1_3Eu**, as the ΔJ = 2, is highly sensitive to the change in the local coordination environment of Eu(III) ion.[22]

Having successfully formed **1_3Eu** and **2_3Eu**, and analyzed their luminescent properties in solution, the self-assembling properties of **1_3Eu** and **2_3Eu** were further investigated at an air-water interface by forming Langmuir films. Only a small numbers of examples of Langmuir-Blodgett films made from kinetically and thermodynamically stable lanthanide complexes have been reported to date.[23-38] Furthermore, only a few examples of CPL Langmuir-Blodgett films have been made,[28] and to the best of our knowledge, no examples of CPL lanthanide emitting Langmuir-Blodgett films have been reported to date. The Langmuir films of **1_3Eu** and **2_3Eu** were identified by monitoring the pressure-area isotherms; where the exponential increase in surface pressure indicated transition from liquid-expanded phases to liquid-condensed and solid phases, as shown in Figure 3.[39] These films were seen to collapse at 34 mN m^{-1} for **1_3Eu** and at 29 mN m^{-1} for **2_3Eu**, corresponding to areas of *ca.* 75±5 Å^2. These areas are approximately those expected for three alkyl chains (~66 Å^2 per molecule),[40,41] and are in agreement with the complexes remaining intact at the air-water interface with supramolecular organization of **1_3Eu** and **2_3Eu**, as monolayers. Excellent stability properties were exhibited by films of both complexes with no pressure decrease observed on keeping the films at the liquid-condensed phase for an extended period of time (>1 hour, inset Figure 3). The transfer of the **1_3Eu** and **2_3Eu** films onto quartz slides was next undertaken, and the formation of Langmuir-Blodgett monolayers was confirmed, where the monolayers were transferred with high transfer ratios (TR = ~1) on the *emersion* of the quartz support. The exact structural nature of these films is currently under investigation, however, we can assume that the polar Eu(III) coordination sphere is orientated towards the water phase and the hexadecyl chains pointing out, as attempts to transfer these films by *immersion* was not successful. Having successfully formed Langmuir-Blodgett films of **1_3Eu** and **2_3Eu**, their photophysical properties were next evaluated, by recording their UV-Vis absorption, phosphorescence and excitation spectra (See Supporting Information Fig. S16 and S17 for **1_3Eu** and **2_3Eu**, respectively). The UV-Vis absorption spectra matched that seen for these complexes when recorded in solution (cf. Figure S12 and S13 Supporting Information), and the phosphorescence excitation spectra (λ_{em} = 620 nm) of both films structurally matched the absorption spectra. The fluorescence emission from these films was however poor, as had been the case when the fluorescence emission of **1_3Eu** and **2_3Eu** was recorded in solution. However, upon excitation of the antenna, both monolayers exhibited time delayed lanthanide luminescence, see Figure 4 for **1_3Eu** (see also Supporting Information Fig. S12 and S13). For these, the Eu(III) emission bands observed at 593, 615 nm and 695 nm were particularly intense as had been seen in solution. These films have been found to be stable under ambient conditions over a period of many months. Furthermore, multiple layers of these films could be transferred onto a quarts slide as demonstrated as an inset in Figure 4, for **1_3Eu**, where the emission from a slide following the deposition of the second monolayer gave rise to enhanced Eu(III) centered luminescence. The excited-state decay of Eu(III) centered emission was also determined, and was found to be similar to that observed in H_2O (See Supporting Information Table S2).

The enantiomeric relationship between the monolayers of **1_3Eu** and **2_3Eu** was also probed using CD and CPL spectroscopies. Unfortunately, we were unable to record the CD spectra of these monolayers, most likely due to low concentration. However, and more importantly, as can be seen in Figure 4 both films gave rise to Eu(III) centered CPL, where the films gave spectra of equal and opposite signs for ΔJ = 1, 2, and 4; these being most pronounced for the ΔJ = 1 and 2 (as was seen in solution for **1_3Eu** and **2_3Eu**), the former being magnetic dipole allowed and as such gave rise to large circular polarization. These results thus clearly confirm that the films formed are chiral and that the Eu(III) centres again report the nature of the chiral environment of the local environment. From these spectra, for **1_3Eu** the dissymmetric factor was determined as g_{lum} = -0.161 and 0.068 for ΔJ = 1 and 2, respectively. This slight difference from the solution studies above is most likely related to the formation of the Langmuir-Blodgett films where the packing of the molecules could have had an effect on the local coordination of the lanthanide ion and/or that this may be due to the effect of the solid surface.

In conclusion, we have developed novel chiral europium directed, luminescent self-assemblies. These amphiphilic molecules

were studied in solutions, as well as used in the formation of stable self-assembled monolayers at an air-water interface. By transferring these monolayers onto quartz slides forming Langmuir-Blodgett films, we were able to generate Eu(III) luminescent monolayers, and probe for the first time, the chiral emission from such films using CPL. These self-assemblies represent the first examples of lanthanide CPL emitting amphiphilic self-assemblies; an exciting area or research we are currently investigating.

Received: ((will be filled in by the editorial staff))
Published online on ((will be filled in by the editorial staff))

Keywords: Chiral · Luminescence · Lanthanide · Langmuir-Blodgett · Surface

[1] S. Brooker, J. A.Kitchen, *Dalton Trans.* **2009**, 7331-7340.
[2] S. V. Eliseeva, J.-C. G. Bünzli, *Chem. Soc. Rev.* **2010,** *39*, 189-227.
[3] O. Ikkala, ten G. Brinke, *Science* **2002,** *295*, 2407-2409.
[4] L.-M. Xu, X. Chen, K.-Z. Yang, *Curr. Top. Colloid Interface Sci.* **2003,** *6*, 113-119.
[5] a) S. V. Eliseeva, J.-C. G. Bünzli, *Chem. Soc. Rev.*, **2010**, *39*, 189-227. b) K. Binnemans, *Chem. Rev.* **2009,** *109*, 4283-4374.
[6] C. Benelli, D. Gatteschi, *Chem. Rev.* **2002,** *102*, 2369-2387.
[7] M. H. Keefe, K. D. Benkstein, J. T. Hupp, *Coord. Chem. Rev.* **2000,** *205*, 201-228.
[8] D. Parker, R. S. Dickins, H. Puschmann, C. Crossland, J. A. K. Howard, *Chem. Rev.* **2002,** *102*, 1977-2010.
[9] a) S. Faulkner, L. S. Natrajan, W. S. Perry, D. Sykes, *Dalton Trans*. **2009**, 3890-3899b) M. D. Ward, *Coord. Chem. Rev.* **2007,** *251*, 1663-1677.
[10] S. M. Goldup, D. A. Leigh, P. J. Lusby, R. T. McBurney, A. M. Z. Slawin, *Angew. Chem. Int. Ed.* **2008,** *47*, 6999.
[11] a) A. J. Prikhod'ko, F. Durola, J. P. Sauvage, *J. Am. Chem. Soc.* **2008,** *130*, 448. b) K. S. Chichak, S. J. Cantrill, A. R. Pease, S.-H. Chui, G. W. V. Cave, J. L. Atwood, J. F. Stoddart, *Science* **2004,** *304*, 1308.
[12] a) C. M. G. dos Santos, A. J. Harte, S. J. Quinn, T. Gunnlaugsson, *Coord. Chem. Rev*., **2008**, *252*, 2512. b) J. P. Leonard, C. B. Nolan, F. Stomeo, T. Gunnlaugsson, *Top. Curr. Chem.*, **2007**, *281*, 1. c) S. E. Plush, T. Gunnlaugsson. *Org. Lett*. **2007**, *9*, 1919. d) S. J. A. Pope, B. J. Coe, S. Faulkner, E. V. Bichenkova, X. Yu, K. T. Douglas, *J. Am. Chem. Soc*. **2004**, *126*, 9490. e) T. Lazarides, D. Skykes, S. Faulkner, A. Barbieri, M. D.Ward, *Chem. Eur. J.* **2008**, *14*, 9389. f) T. Lazarides, S. G. Baca, S. J. A. Pope, H. Adams, M. D. Ward, *Inorg. Chem*. **2008**, *47*, 3736.
[13] a) C. Butler, S. Goetz, C. M. Fitchett, P. E. Kruger, T. Gunnlaugsson, *Inorg. Chem*., **2011**, *50*, 2723. b) M. Cantuel, C. Lincheneau, T Buffeteau, L. Jonusauskaite, T. Gunnlaugsson, G. Jonusauskas, N. McClenaghan, *Chem. Commun*. **2010**, *46*, 2486 c) A. M. Nonat, S. J. Quinn, T. Gunnlaugsson, *Inorg. Chem*. **2009**, 48, 1646. d) A. M. Nonat, A. J. Harte, K. Sénéchal-David, J. P. Leonard, T. Gunnlaugsson, *Dalton Trans.* **2009**, 4703. e) T. Riis-Johannessen, G. Bernardinelli, Y. Filinchuk, S. Clifford, N. D. Favera, C. Piguet, *Inorg. Chem*., **2009**, *48*, 5512-5525.
[14] a) C. Piguet, *Chem Commun*, **2010**, *46*, 6209-6231. b) J.-C. G. Bünzli, *Chem. Rev*., **2010**, *110*, 2729-2755. c) J.-C. G. Bünzli, *Acc. Chem. Res.* **2006,** *39*, 53-61. d) J.-C. G. Bünzli, C. Piguet, *Chem. Soc. Rev*. **2005,** *34*, 1048-1077.
[15] a) J. Hamacek, C. Besnard, T. Penhouet, P. Y. Morgantini, *Chem. Eur. J.* **2011**, *17*, 6753-6764. b) G. Canard, S. Koeller, G. Bernardinelli, C. Piguet, *J. Am. Chem. Soc.*, **2008**, *130*, 1025. c) A.-S. Chauvin, S. Comby, B. Song, C. D. B. Vandevyver, J.-C. G. Bünzli, *Chem. Eur. J.* **2008,** *14*, 1726-1739. d) S. Torelli, D. Imbert, M. Cantuel, G. Bernardinelli, S. Delahaye, A. Hauser, J.-C. G. Bünzli, C. Piguet, *Chem. Eur. J*. **2005**, *11*, 3228.
[16] a) B. El Aroussi, S. Zebret, C. Besnard, P. Perrottet, J. Hamacek, *J. Am. Chem. Soc.*, **2011**, *133*, 10764. b) M. Han, H.-Y. Zhang, L.-X Yang, Q. Jiang, Y. Liu, *Org. Lett.*, **2008**, *10*, 5557-5560. c) M. Albrecht, O. Osetska, R. Frehlich, J.-C. G. Bünzli, A. Aebischer, F. Gumy, J. Hamacek, *J. Am. Chem. Soc.* **2007,** *129*, 14178.
[17] J. A. Kitchen, C. Gandolfi, M. Albrecht, G. N. L. Jameson, J. L. Tallon, S. Brooker, *Chem. Commun.* **2010**, 46, 6464-6466.
[18] a) C. Lincheneau, J. P. Leonard, T. McCabe, T. Gunnlaugsson, *Chem. Commun.*, **2011**, 47, 7119-7121. b) J. P. Leonard, P. Jensen, T. McCabe, J. E. O'Brien, R. D. Peacock, P. E. Kruger, T. Gunnlaugsson, *J. Am. Chem. Soc.* **2007,** *129*, 10986-10987.
[19] a) F. Stomeo, C. Lincheneau, J. P. Leonard, J. E. O'Brien, R. D. Peacock, C. P. McCoy, T. Gunnlaugsson, *J. Am. Chem. Soc.* **2009,** *131*, 9636-9637. b) S. Comby, F. Stomeo, C. P. McCoy, T. Gunnlaugsson, *Helv. Chim. Acta* **2009,** *92*, 2461-2473.
[20] C. Lincheneau, R. D. Peacock, T. Gunnlaugsson, *Chem. Asian J.* **2010,** *5*, 500-504.
[21] a) S. Comby, T. Gunnlaugsson, *ACS Nano*, **2011**, *5*, DOI: 10.1021/nn201992z. b) J. Massue, S. J. Quinn, T. Gunnlaugsson, *J. Am. Chem. Soc.*, **2008**, *130*, 6900. c) C. S. Bonnet, J. Massue, S. J. Quinn, T. Gunnlaugsson, *Org. Biomol. Chem*. **2009**, *7*, 3074. d) N. S. Murray, S. P. Jarvis, T. Gunnlaugsson, *Chem. Commun*., **2009**, 4959.
[22] a) G. Muller, *Dalton Trans*., **2009**, 9692-9707. b) J. Gregolinski, P. Starynowicz, K. T. Hua, J. L. Lunkley, G. Muller, J. J. Lisowski, *Am. Chem.. Soc.*, **2008**, *130*, 17761.
[23] H. Lemmetyinen, E. Vuorimaa, A. Jutila, V-. M. Mukkala, H. Takalo, J. Kankare, *Luminescence* **2000**, 15, 341–350.
[24] B. Yan, B. Xu, *J Fluoresc* **2009**, 19, 663-671.
[25] D- J. Qian, K- Z. Yang, H. Nakahara, K. Fukuda, *Langmuir* **1997**, 13, 5925-5932.
[26] P. J. Dutton, L. Conte, *Langmuir* **1999,** *15*, 613-617.
[27] T. Ito, H. Yashiro, T. Yamase, *J Clust Sci* **2006**, 17, 375-397.
[28] J. M. Huttunen, M. Virkki, M. Erkintalo, E. Vuorimaa, A. Efimov, H. Lemmetyinen, M. Kauranen, *J. Phy. Chem. Lett* **2010**, 1, 1826-1829.
[29] X- M. Xiang, D- J. Qian, F- Y. Li, H- T. Chen, H- G. Liu, W. Huang, X- S. Feng, *Colloid Surface A* **2006**, 273, 29-34.
[30] J. Wang, H. Wang, Z. Wang, Y. Yin, F. Liu, H. Li, L. Fu, H. Zhang, *J. Alloy Compd* **2004**, 365, 102.
[31] T. Ito, T. Yamase, *J. Alloy Compd* **2006**, 408, 813.
[32] F. L. Sousa, A. S. Ferreira, R. A. S. Ferreira, A. M. V. Cavaleiro, L. D. Carlos, H. I. S. Nogueira, T. Trindade, *J. Alloy Compd* **2004**, 374, 371.
[33] J. Wang, H. Wang, L. Fu, F. Liu, H. Zhang, *Thin Solid Films* **2002**, 415, 242.
[34] B. Xu, H-X. Zhu, B. Yan, *Inorg. Chem. Comm.* **2010**, *13*, 1448-1450.
[35] B. Xu, B. Yan, *Colloid Surface A* **2008**, 329, 7-11.
[36] K. Binnemans, C. Görller-Walrand, *Chem. Rev.* **2002**, *102*, 2303-2345.
[37] B. Yan, B. Xu, *Appl. Surf. Sci.* **2008**, *254*, 7237-7242.
[38] M. Hasegawa, S. Kunisaki, H. Ohtsu, Werner, F. *Monatsh. Chem.* **2009**, *140*, 751-763.
[39] M. C. Petty, *Langmuir-Blodgett Films: An Introduction*. Cambridge University Press: Cambridge, 1996.
[40] R. Johann, D. Vollhardt, *Mat. Sci. Eng. C* **1999,** *8-9*, 35-42.
[41] D. K. Chattoraj, E. Halder, K. P. Das, A. Mitra, *Adv. Colloid Interfac.* **2000,** *123–126*, 151.

Entry for the Table of Contents

Chiral Lanthanide Emissive LB Films

Jonathan A. Kitchen*, Dawn E. Barry, Laszlo Mercs, Martin Albrecht, Robert D. Peacock, and Thorfinnur Gunnlaugsson* _____ **Page – Page**

Circular polarized lanthanide luminescence from Langmuir-Blodgett films formed from optically active and amphiphilic Eu(III) based self-assembly complexes

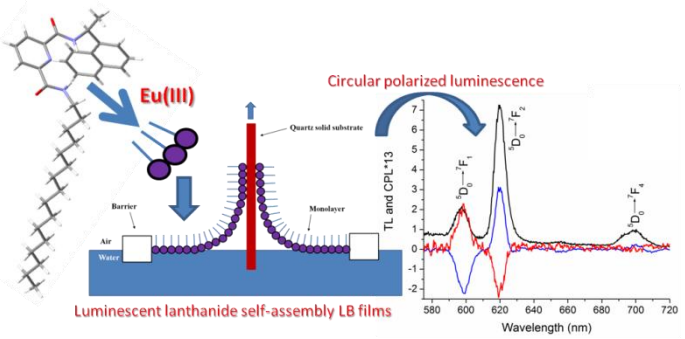

The development of chiral amphiphilic self-assembled complexes 1_3Eu and 2_3Eu by using Europium(III) directed synthesis is described. These systems form stable Langmuir-Blodgett (LB) films on quartz slides resulting in stable monolayers that exhibit the first example of time delayed Eu(III) centered emission and circular polarized luminescence (CPL) upon from a LB film.

Supporting Information

Experimental details

General remarks

All chemicals were purchased from commercial sources and used as received. Solvents were HPLC grade and were used without further purification. Elemental analyses were carried out at the Microanalytical Laboratory, School of Chemistry and Chemical Biology, University College Dublin. Infrared spectra were recorded on a Perkin-Elmer-Spectrum-One FT-IR spectrometer equipped with a Universal-ATR sampling accessory; solid samples were recorded directly as neat samples; in cm^{-1}. NMR data were recorded on a Bruker-DPX-400-Avance spectrometer (400.13 (^{1}H) and 100.6 MHz (^{13}C)) or a Bruker-AV-600 spectrometer (600.13 (^{1}H) and 150.2 MHz (^{13}C)), in commercially available deuterated solvents; δ in ppm relative to $SiMe_4$ (= 0 ppm) referenced relative to the internal solvent signals, J in Hz; data were processed with Bruker Win-NMR 5.0 and Topspin 2.1 softwares.

Circular dichroism (CD) spectra were recorded in CH_3CN on a Jasco J-810-150S spectropolarimeter. Emission spectra and lifetime measurements were measured with a Varian-Cary-Eclipse luminescence spectrometer. In a typical spectrophotometric titration, 3.0 ml of ligand **1** or **2** at a concentration of 1.0×10^{-5} $molL^{-1}$ was titrated with a ca. 5×10^{-4} $molL^{-1}$ Eu(III) solution.

Circularly polarised luminescence (CPL) spectra were recorded by Dr. R. Peacock at the University of Glasgow. Excitation of Eu(III) (560-581nm) was accomplished by using a Coherent 599 tuneable dye laser (0.03 nm resolution) with argon ion laser as a pump source. Calibration of the emission monochromator was accomplished by passing scattered light from a low power He-Ne laser through the detection system. The optical detection system consisted of a photoelastic modulator (PEM, Hinds Int.) operating at 50 kHz and a linear polariser, which together act as a circular analyser, followed by a long pass filter, focusing lens and a 0.22 m double monochromator. The emitted light was detected by a cooled EM1-9558QB photomultiplier tube operating in photon counting mode. The 50 KHz reference signal from the photoelastic modulator was used to direct the incoming pulses into two separated counters. An up counter, which counts every photon pulse and thus is a measure of the total luminescence signal $I = I_{left} + I_{right}$, and an up/down counter, which adds pulses when the analyser is transmitting to the left circularly polarised light and subtracts pulses when the analyser is transmitting right circularly polarised light. The second counter provides a measure of the differential emission intensity $\Delta I = I_{left} - I_{right}$.

Complexation reactions were carried out in 2-5 mL Biotage Microwave Vials in a Biotage Initiator Eight EXP microwave reactor. Reactions were performed at 70 °C for 10 minutes in HPLC grade methanol.

Pressure–area isotherms and time stability were measured at 25°C on a KSV MiniMicro Langmuir-Blodgett trough (KSV, Finland) with a surface area between 1700 and 8700 mm^2. Water was purified with a Milli-Q® Integral system (Millipore), and its resistivity was measured to be higher than 18 MΩ cm. Chloroform (puriss. p.a. ≥ 99.8%, Sigma-Aldrich) was used as spreading solvent for the ligands; a 9:1 mixture of chloroform/MeOH for $[Eu^{III}(\mathbf{L})_3](CF_3SO_3)_3$. Typically drops (20 µl) of the surfactant solution (~0.25 mM) were deposited using a microsyringe on the water subphase. After leaving the solvent to evaporate for 20 min, the barriers were compressed at 6 mm min^{-1} (3 cm^2 min^{-1}) and the surface pressure was monitored using a platinum Wilhelmy plate.

X-ray data (Table S1) was collected on a Rigaku Saturn 724 CCD Diffractometer using graphite-monochromated Mo-Kα radiation (λ = 0.71073 Å). The data was collected using Crystalclear-SM 1.4.0 software. Data integration, reduction and correction for absorption and polarization effects were all performed using Crystalclear-SM 1.4.0 software. Space group determination was obtained using Crystal structure ver. 3.8. The structure was solved by direct methods (SHELXS-97) and refined against all F^2 data (SHELXL-97).[1] All H-atoms, except for N-H protons, were positioned geometrically and refined using a riding model with d(CH_{aro}) =0.95 Å, *U*iso = 1.2*U*eq (C) for aromatic, d(CH) =1.0 Å, *U*iso = 1.2*U*eq (C) for CH, 0.99 Å, *U*iso = 1.2*U*eq (C) for CH_2 and 0.98 Å, *U*iso = 1.2*U*eq (C) for CH_3. Amide N-H protons were found from the difference map and fixed to the attached atoms with $U_H = 1.2U_N$.

*Synthesis of N_2-[1-hexadecyl]-N_6-[(1R or S)-1-(naphthalen-1-yl)ethyl]pyridine-2,6-dicarboxamides (**1** and **2**)*

N_6-(1(R)-Naphthalen-1-yl-ethylcarbamoyl)-pyridine-2-carboxylic acid (**3**) (0.5 g, 1.5 mmol) and HOBt (0.21 g, 1.5 mmol) were added to THF (20 mL) and put under argon. Hexadecylamine (0.377 g, 1.5 mmol) and Et_3N (0.23 mL, 1.6 mmol) were added and the orange solution cooled to 0 °C before EDCI·HCl (0.315 g, 1.6 mmol) was added. After one hour the mixture was allowed to warm to room temperature and stirring was continued for 36 hours. THF was removed *in vacuo* to give an orange oil that was subsequently taken up in DCM, washed with 1M HCl (4 x 20 mL), $NaHCO_3$ (2 x 20 mL), water (1 x 20 mL) and brine (20 mL). The DCM layer was dried over Na_2SO_4. Removal of DCM yielded N_2-[1-hexadecyl]-N_6-[(1*R*)-1-(naphthalen-1-yl)ethyl]pyridine-2,6-dicarboxamide (**1**) as a pale orange oil (606 mg, 74%). ^{1}H-NMR (400 MHz, $CDCl_3$, 298 K): δ 8.37 (d, J = 7.8 Hz, 1H, pyr-*H*), 8.28 (d, J = 7.8 Hz, 1H, pyr-*H*), 8.25 (d, J = 8.5 Hz, 1H, N*H*), 8.17 (d, J = 8.5 Hz, 1H, N*H*), 7.95 (t, J = 7.8 Hz, 1H, pyr-*H*), 7.83 (d, J = 7.8 Hz, 1H, nap-*H*), 7.76 (m, 2H, nap-*H*), 7.52 (m, 3H, nap-*H*), 7.38 (t, J = 7.8 Hz, 1H, nap-*H*), 6.11 (q, J = 7.3 Hz, 1H, MeC*H*), 3.33 (m, 1H NH-CH_2), 3.25 (m, 1H NH-CH_2), 1.78 (d, J = 6.8 Hz, 3H, CHCH_3), 1.47 (t, J = 6.6 Hz, 2H, NHCH_2CH_2), 1.28 (s, 26H, 13×CH_2), 0.90 (t, J = 6.6, 3H, CH_2CH_3). ^{13}C-NMR (100 MHz, $CDCl_3$, 298 K): δ 163.3 (CO), 162.7 (CO), 148.9 (C), 148.6 (C), 138.8 (CH), 138.0 (C), 133.9 (C), 131.1 (C), 128.9 (CH), 128.4 (CH), 126.6 (CH), 125.9 (CH), 125.1 (CH), 125.0 (CH), 125.0 (CH), 123.4 (CH), 122.8 (CH), 45.3 (CH), 39.6 (CH_2), 31.9 (CH_2), 29.7-29.3 (11×CH_2), 26.9 (CH_2), 22.7 (CH_2), 20.9 (CH_3), 14.1 (CH_3) ppm. IR(neat): 3303, 2922, 2852, 1650 (C=O), 1523, 1443, 1375, 1310, 1238, 1173, 1118, 1075, 999, 845, 799, 776, 741, 721, 676 cm^{-1}. HR-ESI-MS: 566.3720 ($[M+Na]^+$, $C_{35}H_{49}N_3O_2Na^+$; calc. 566.3722).

N_6-(1(S)-Naphthalen-1-yl-ethylcarbamoyl)-pyridine-2-carboxylic acid (**4**) (0.37 g, 1.05 mmol) and HOBt (0.142 g, 1.05 mmol) were added to THF (20 mL) and put under argon. Hexadecylamine (0.254 g, 1.05 mmol) and Et_3N (0.154 mL, 1.10 mmol) were added and the orange solution cooled to 0 °C before EDCI·HCl (0.211 g, 1.10 mmol) was added. After one hour the mixture was allowed to warm to room temperature and stirring was continued for 24 hours. THF was removed *in vacuo* to give an orange oil that was subsequently taken up in DCM, washed with 1M HCl (4 x 20 mL), $NaHCO_3$ (2 x 20 mL), water (1 x 20 mL) and brine (20 mL). The DCM layer was dried over Na_2SO_4. Removal of DCM yielded N_2-[1-hexadecyl]-N_6-[(1*S*)-1-(naphthalen-1-yl)ethyl]pyridine-2,6-dicarboxamide (**2**) as a pale yellow oil (322 mg, 82%). ^{1}H-NMR (600 MHz, $CDCl_3$, 298 K): δ 8.38 (d, *J* = 7.8 Hz, 1H, pyr-*H*), 8.30 (d, *J* = 7.68 Hz, 1H, pyr-*H*), 8.19 (d, *J* = 8.52 Hz, 1H, nap-*H*), 7.98 (t, *J* = 7.86 Hz, 1H, pyr-*H*) 7.86 (d, *J* = 7.86 Hz, 1H, nap-*H*), 7.7 (d, *J* = 8.16 Hz, 1H, nap-*H*), 7.59 (d, *J* = 7.14 Hz, 1H, nap-*H*), 7.55 (t, *J* = 6.93 Hz, 1H, nap-*H*), 7.50 (t, *J* = 7.44 Hz, 1H, nap-*H*), 7.42 (t, *J* = 7.5 Hz, 1H, nap-*H*), 6.12 (m, 1H, MeC*H*), 3.38 (m, 1H, NH-CH_2), 3.30 (m, 1H, NH-CH_2), 1.82 (d, *J* = 6.78 Hz, 3H, CHCH_3), 1.49 (m, 2H, NHCH$_2$CH_2), 1.27 (s, 26H, 13×CH_2), 0.9 (t, *J* = 6.9 Hz, 3H, CH$_2$CH_3). ^{13}C-NMR (150 MHz, $CDCl_3$, 298 K): 163.3 (CO), 162.7 (CO), 148.8 (C), 148.6 (C), 138.7 (CH), 138.0 (C), 133.8 (C), 131.0 (C), 128.8 (CH), 128.3 (CH), 126.5 (CH), 125.8 (CH), 125.0 (CH), 124.9 (CH), 124.8 (CH), 123.2 (CH), 122.7 (CH), 45.1 (CH), 39.5 (CH_2), 31.8 (CH_2), 29.6-29.2 (11×CH_2), 26.9 (CH_2), 22.6 (CH_2), 20.8 (CH_3), 14.0 (CH_3). IR(neat): 3309, 2921, 2852, 1654 (C=O), 1524, 1443, 1375, 1237, 1074, 999, 844, 798, 776, 722, 677 cm^{-1}. HR-ESI-MS: 566.3722 ([M+Na]$^+$, $C_{35}H_{49}N_3O_2Na^+$; calc. 566.3722).

Synthesis of Eu(III) complexes ***1$_3$Eu*** *and* ***2$_3$Eu****:*

General procedure

1 or **2** (30 mg, 0.06 mmol) in 5 mL MeOH had solid $Eu(CF_3SO_3)_3$ (18 mg, 0.03 mmol) added and was heated at 70 °C under microwave irradiation for 10 minutes. The resulting clear yellow solutions were subjected to vapour diffusion of diethyl ether resulting in white solids.

[Eu(**1**)$_3$]$(CF_3SO_3)_3$ (**1$_3$Eu**), white solid, 22 mg (42%). Elemental analysis for $C_{108}H_{147}N_9O_{15}F_9S_3Eu$ (2229.92 gmol^{-1}) calc: C 58.15, H 6.64, N 5.65; found C 57.16, H 6.31, N 5.55%. IR(neat): 3274, 3100, 2924, 2854, 1634 (C=O), 1595, 1558, 1457, 1275, 1241, 1225, 1197, 1163, 1030, 839, 801, 779, 752, 721, 661 cm^{-1}. HR-MALDI-MS: 1537.5897 ([M-L-CF_3SO_3]$^+$, $C_{72}H_{98}N_6O_{10}F_6S_2Eu^+$; calc 1537.5903).

[Eu(**2**)$_3$]$(CF_3SO_3)_3$ (**2$_3$Eu**), white solid, 21 mg (40%). Elemental analysis for $C_{108}H_{147}N_9O_{15}F_9S_3Eu$ (2229.92 gmol^{-1}) calc: C 58.15, H 6.64, N 5.65; found C 57.99, H 6.50, N 5.58%. IR(neat): 3284, 2920, 2852, 1633 (C=O), 1594, 1560, 1459, 1242, 1187, 1165, 1029, 839, 801, 779, 753, 720 cm^{-1}. HR-MALDI-MS: 1537.5876 ([M-L-CF_3SO_3]$^+$, $C_{72}H_{98}N_6O_{10}F_6S_2Eu^+$; calc. 1537.5903).

Figures and Tables

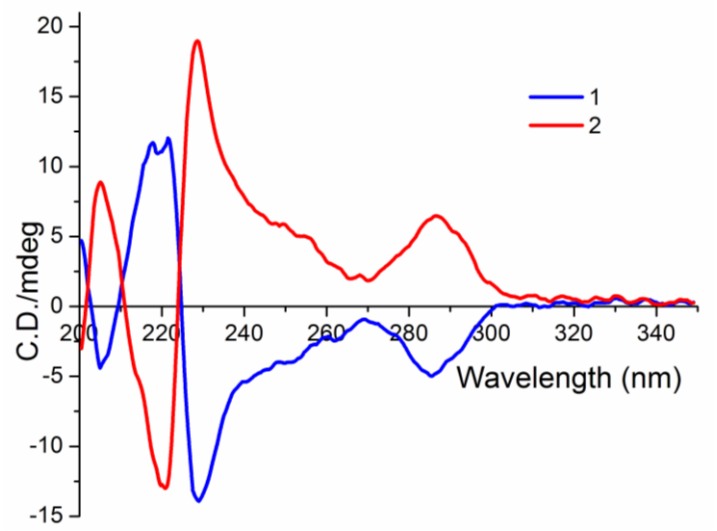

Figure S1: CD spectra of **1** (blue) and **2** (red) in MeCN.

Table S1: Crystal data and structure refinement for **1**.

CCDC entry	814658	
Empirical formula	$C_{35}H_{49}N_3O_2$	
Formula weight	543.77	
Temperature	108(2) K	
Wavelength	0.71073 Å	
Crystal system	Monoclinic	
Space group	P2(1)	
Unit cell dimensions	a = 11.246(2) Å	a= 90°.
	b = 17.766(4) Å	b= 95.11(3)°.
	c = 16.042(3) Å	g = 90°.
Volume	3192.4(11) $Å^3$	
Z	4	
Density (calculated)	1.131 Mg/m^3	
Absorption coefficient	0.070 mm^{-1}	
F(000)	1184	
Crystal size	0.60 x 0.20 x 0.20 mm^3	
Theta range for data collection	1.71 to 24.50°.	
Index ranges	-13<=h<=13, -17<=k<=20, -18<=l<=18	
Reflections collected	24917	
Independent reflections	5505 [R(int) = 0.1072]	
Completeness to theta = 24.50°	99.9 %	
Absorption correction	Semi-empirical from equivalents	
Max. and min. transmission	0.9862 and 0.9593	
Refinement method	Full-matrix least-squares on F^2	
Data / restraints / parameters	5505 / 1 / 725	
Goodness-of-fit on F^2	1.209	
Final R indices [I>2sigma(I)]	R1 = 0.0899, wR2 = 0.1995	
R indices (all data)	R1 = 0.1077, wR2 = 0.2174	
Largest diff. peak and hole	0.247 and -0.317 $e.Å^{-3}$	

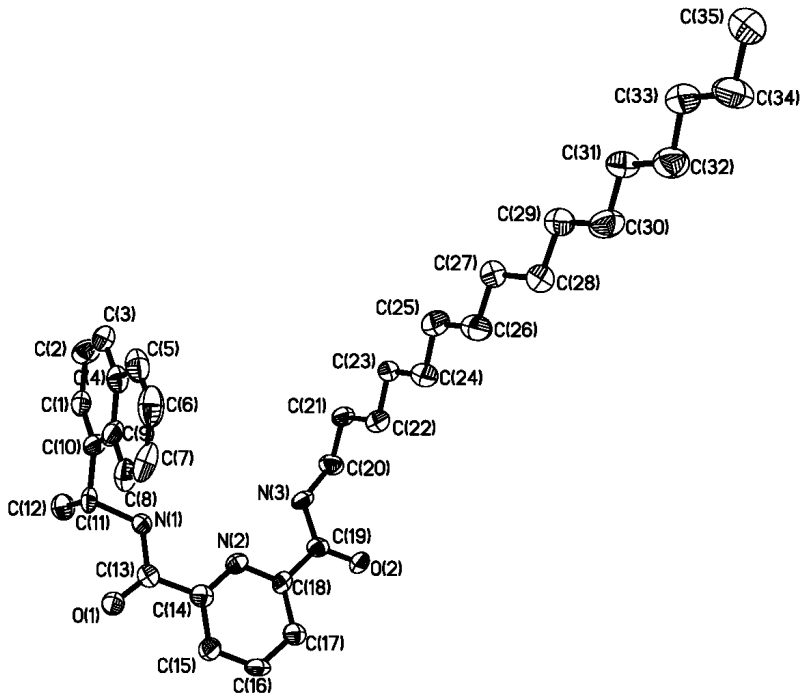

Figure S2: Perspective view of “straight” chain molecule of **1**. Hydrogen atoms have been omitted for clarity.

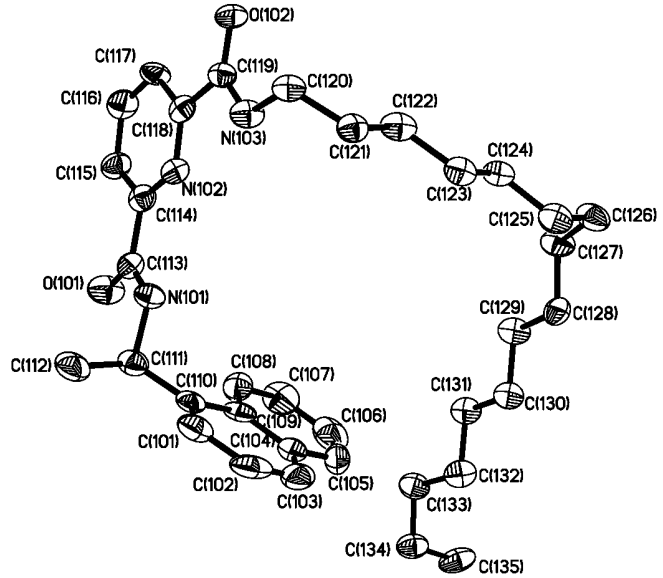

Figure S3: Perspective view of "bent" chain molecule of **1**. Hydrogen atoms have been omitted for clarity.

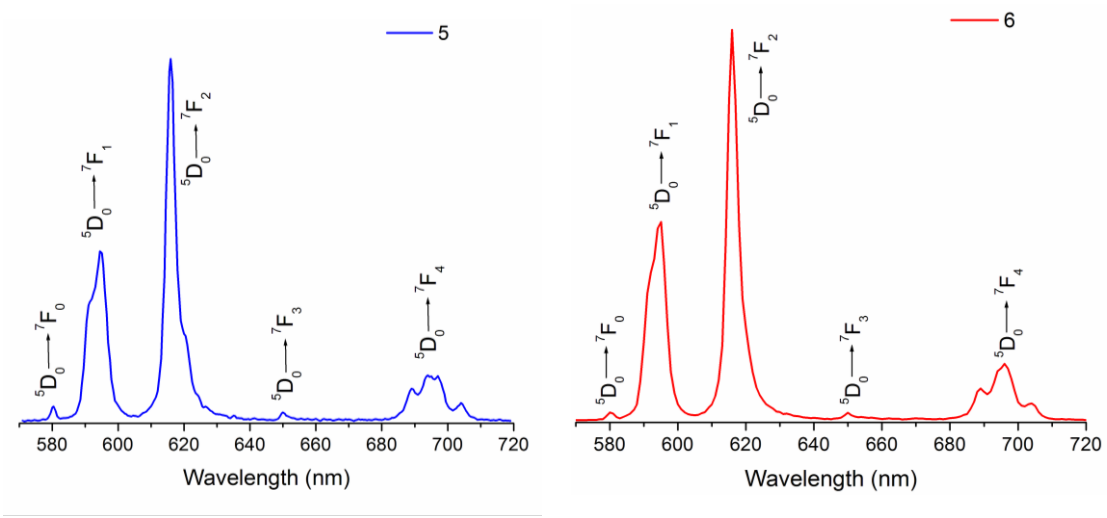

Figure S4: Luminescence spectra of **1_3Eu** (blue) and **2_3Eu** (red) in MeOH at RT.

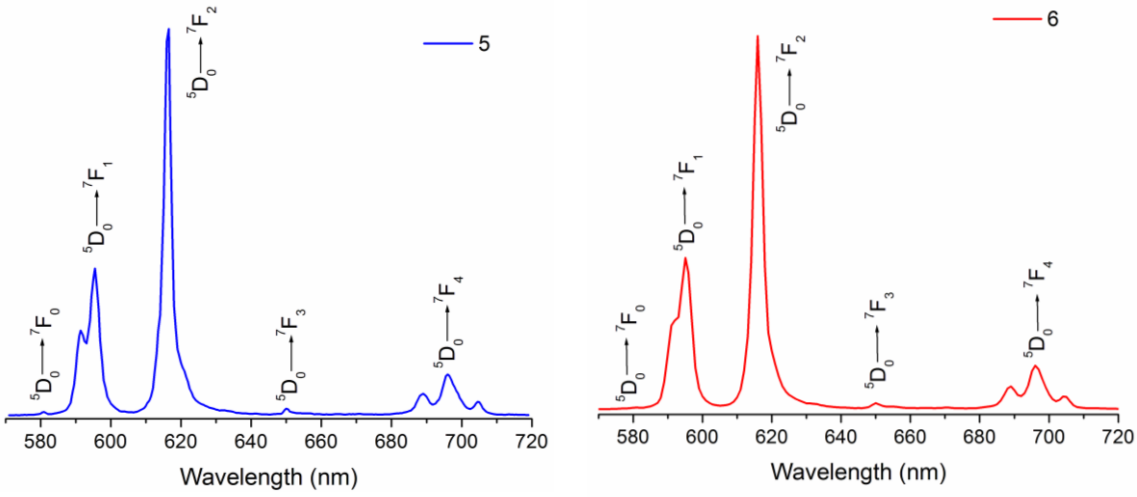

Figure S5: Luminescence spectra of **1_3Eu** (blue) and **2_3Eu** (red) in MeCN at RT.

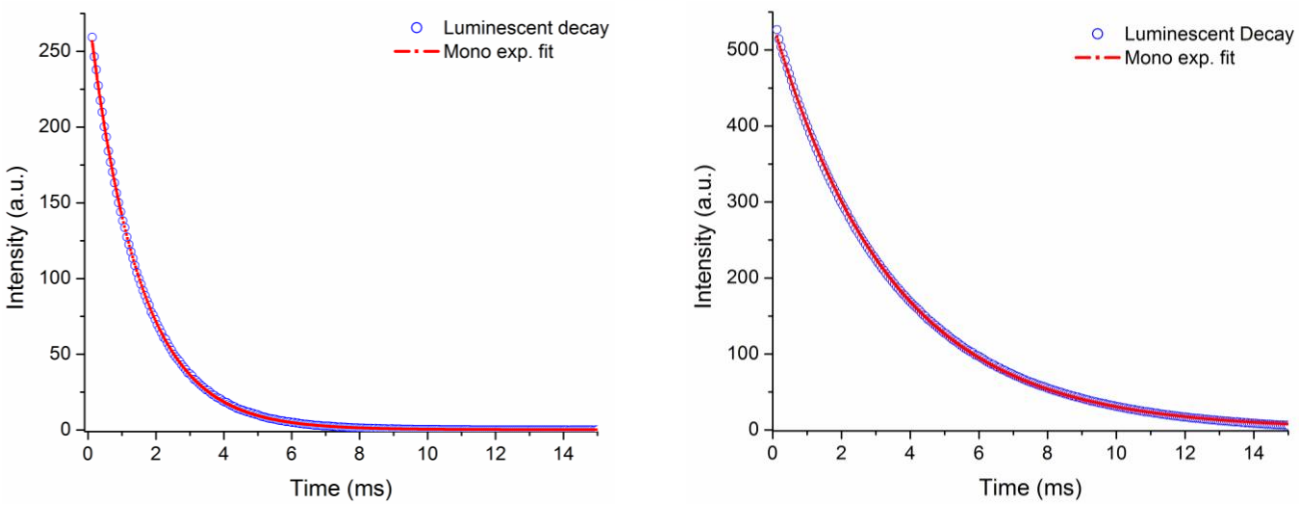

Figure S6: Eu(III) excited state decay of **1_3Eu** in H_2O (left) and D_2O (right) and the observed fitting of the decay.

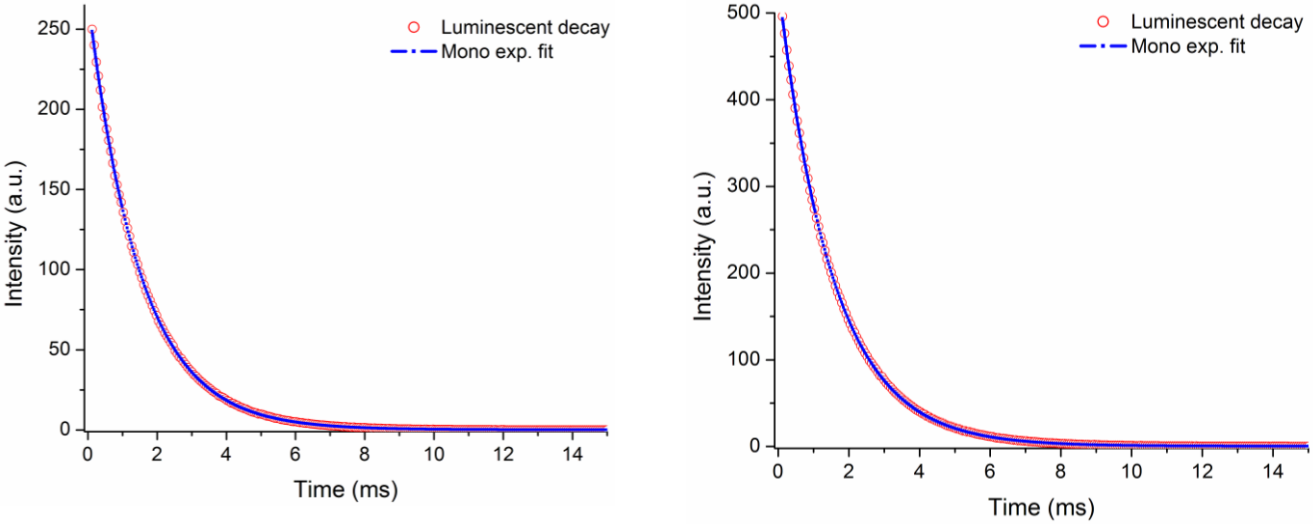

Figure S7: Eu(III) excited state decay of **2_3Eu** in H_2O (left) and D_2O (right) and the observed fitting of the decay.

Table S2: Lifetimes of 1_3Eu and 2_3Eu in H_2O and D_2O and calculated hydration states (q).

	Lifetime (τ_{H2O}) in H_2O (ms)	Lifetime (τ_{D2O}) in D_2O (ms)	Hydration state (q) ±0.5
1_3Eu	1.471	1.603	-0.22
2_3Eu	1.489	1.537	-0.27
Lifetimes of monolayers			
1_3Eu	1.477	0.088	
2_3Eu	1.502	0.350	

q values in water formula: $q = A\,(1/\tau_{H_2O} - 1/\tau_{D_2O} - 0.25)$ with A = 1.2

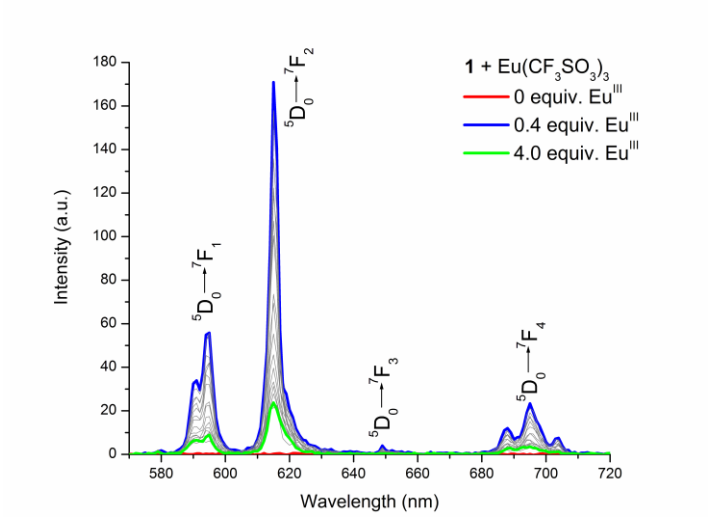

Figure S8: Overall changes in the Eu(III) phosphorescence spectra upon titrating **1** (1×10^{-5}) with $Eu(CF_3SO_3)_3$ in MeCN at RT.

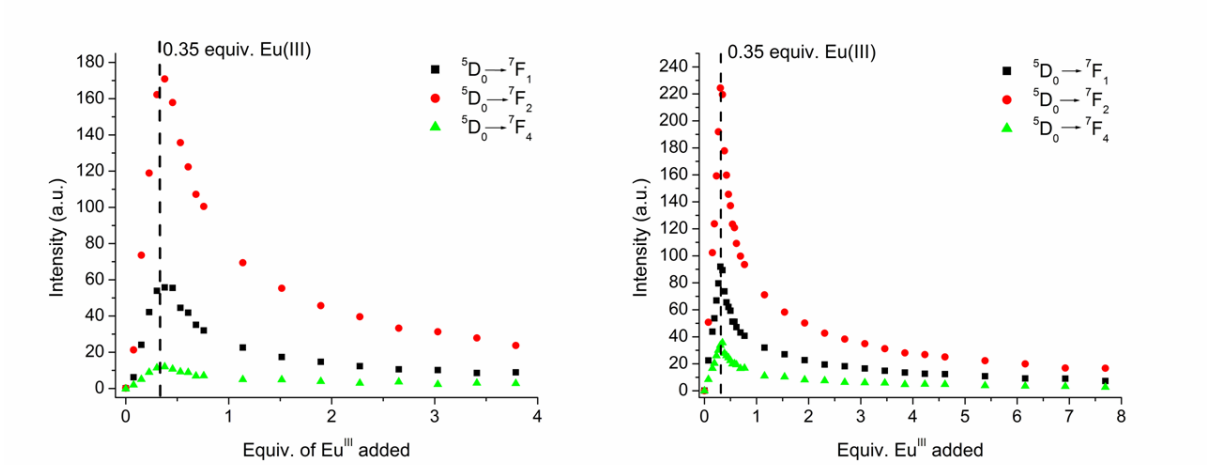

Figure S9: Experimental binding isotherms of the Eu(III) phosphorescence-emission intensities for titration of **1** (left) or **2** (right) at λ 595 ($^5D_0\rightarrow{}^7F_1$), 615 ($^5D_0\rightarrow{}^7F_2$) and 695 nm ($^5D_0\rightarrow{}^7F_4$) vs. the equiv. of $Eu(CF_3SO_3)_3$.

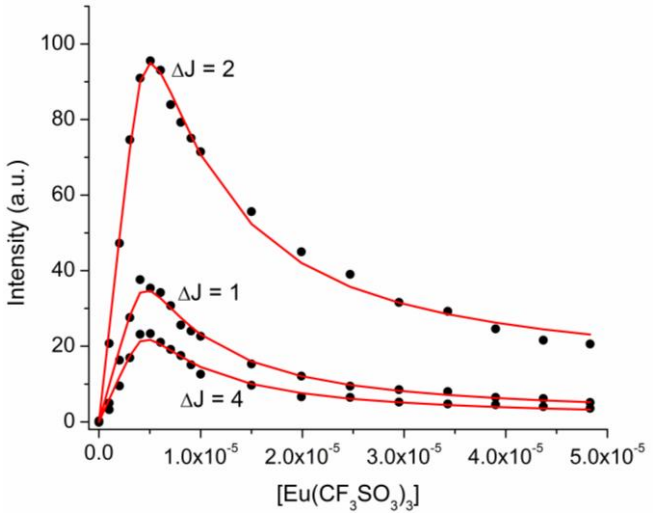

Figure S10: Experimental binding isotherms for the changes in the Eu(III) luminescence spectra upon titrating **1** (1×10^{-5} M) with $Eu(SO_3CF_3)_3$ in MeCN at room temperature and their corresponding fit by means of SPECFIT (—).

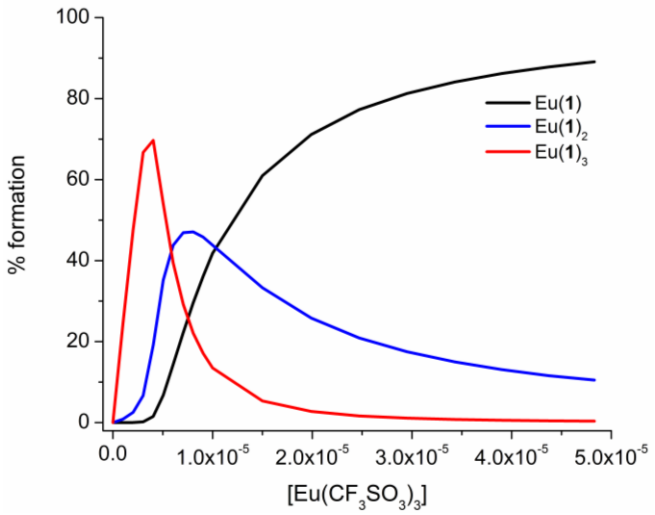

Figure S11: Speciation-distribution diagram obtained from the titration of **1** with $Eu(CF_3SO_3)_3$.

Table S3: Binding constants and % formation of species obtained for **1** and **2** vs Eu(III) from UV-Vis and Luminescence.

UV-vis			**Luminescence**		
Log $\beta_{1:1}$	Log $\beta_{1:2}$	Log $\beta_{1:3}$	Log $\beta_{1:1}$	Log $\beta_{1:2}$	Log $\beta_{1:3}$
6.7 ± 0.2	13.8 (fixed)	20.5 ± 0.3	6.7 ± 0.2	14.3 ± 0.3	21.9 ± 0.4
6.6 ± 0.2	13.8 (fixed)	20.9 ± 0.3	6.7 ± 0.1	13.3 ± 0.2	19.9 ± 0.2
% Formation for M:L = 1:3			% Formation for M:L = 1:3		
-	8	82	-	19	70
-	3	87	-	7	80

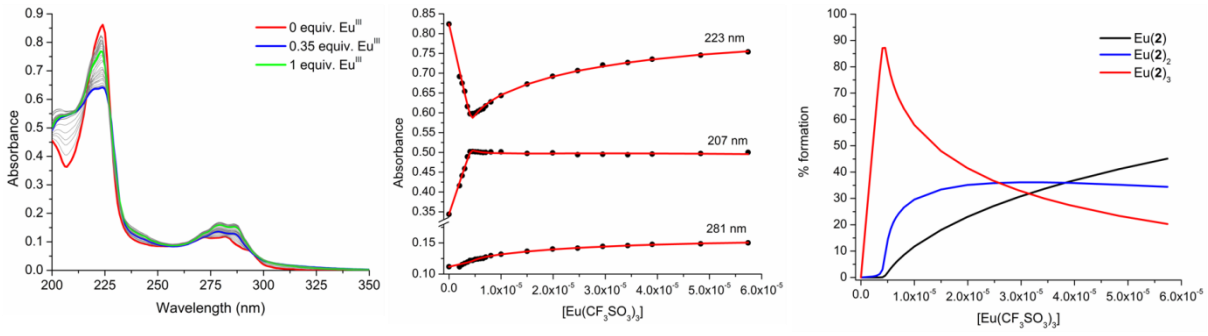

Figure S12: Experimental binding isotherms for the changes in the absorbance spectra upon titrating **1** (1×10^{-5} M) with $Eu(SO_3CF_3)_3$ (0-5 equiv.) in MeCN at RT and their corresponding fit by means of SPECFIT (—) (left). Speciation-distribution diagram obtained from the titration of **1** with $Eu(CF_3SO_3)_3$ (right).

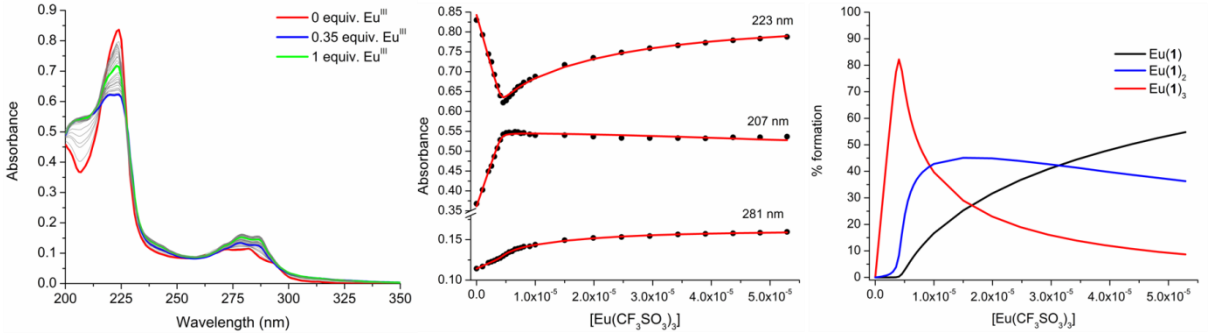

Figure S13: Experimental binding isotherms for the changes in the absorbance spectra upon titrating **2** (1×10^{-5} M) with Eu(SO3CF3)3 (0-6 equiv.) in MeCN at RT and their corresponding fit by means of SPECFIT (—) (left). Speciation-distribution diagram obtained from the titration of **2** with $Eu(CF_3SO_3)_3$ (right).

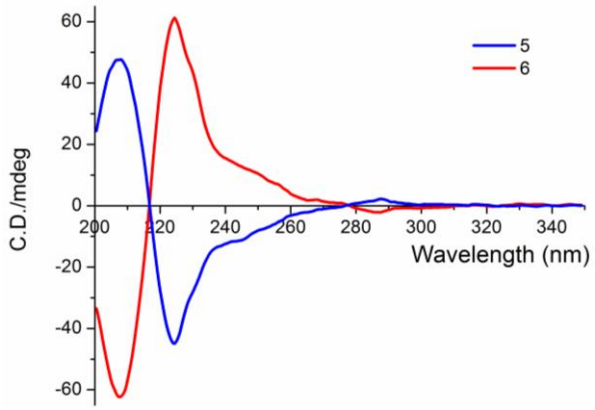

Figure S14: CD spectra of **1_3Eu** (blue) and **2_3Eu** (red) in MeCN.

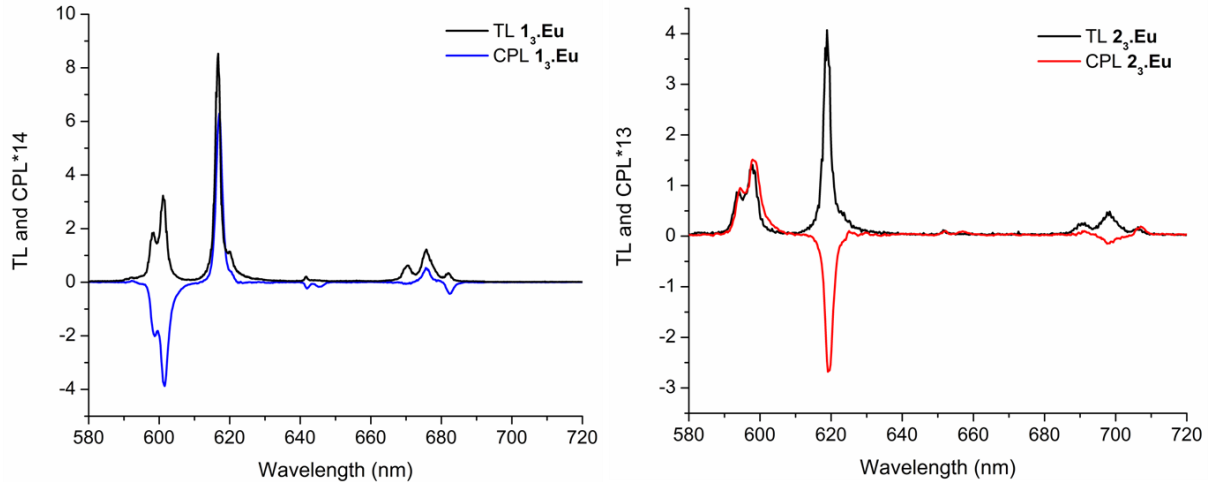

Figure S15: The total Eu(III) emission (black) and CPL (blue) of **1$_3$Eu** (left) and total Eu(III) emission (black) and CPL (red) of **2$_3$Eu** (right).

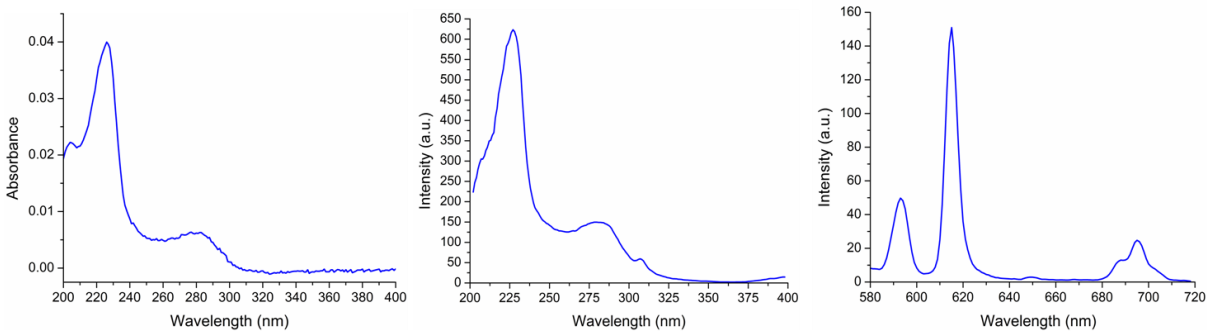

Figure S16: The absorption spectrum (left), the excitation spectrum, λ_{em} = 615 nm (centre) and the phosphorescence emission spectrum, λ_{ex} = 281 nm (right) of **1$_3$Eu** immobilised on a quartz slide.

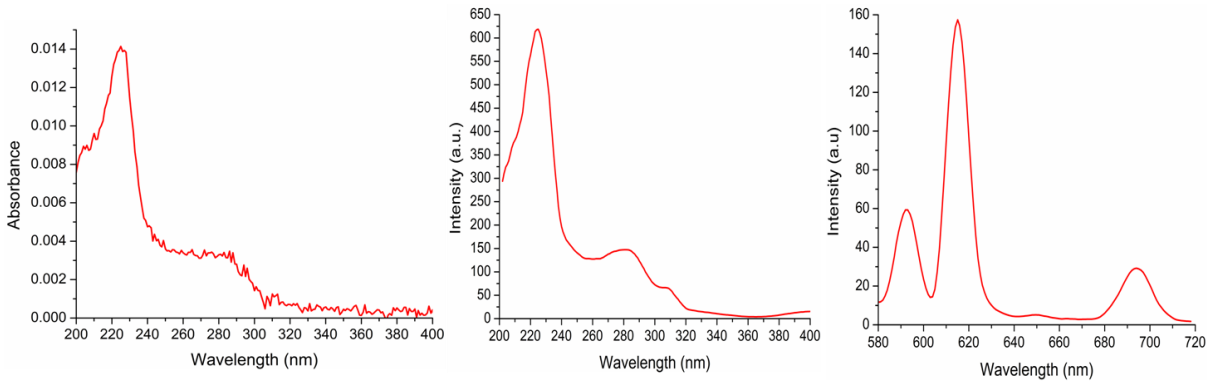

Figure S17: The absorption spectrum (left), the excitation spectrum, λ_{em} = 615 nm (centre) and the phosphorescence emission spectrum, λ_{ex} = 281 nm (right) of **2$_3$Eu** immobilised on a quartz slide.

1. G. M. Sheldrick, *Acta Crystallogr., Sect. A*, 2008, **A64**, 112.